



To be published in Phys.Rev.C

PACS number(s): 25.60.Gc, 21.10.Gv, 25.70.Mn, 27.20.+n, 25.70.Hi

In this paper we study the neutron angular distribution in reactions initiated by  $^{11}Be$ . The neutron angular distribution is obtained from a general formalism which can be applied to any heavy-ion transfer to the continuum reaction at intermediate energies. With the same method momentum distributions can be obtained. Our equations can be reduced to the incident free particle limit and the validity of this approximation is discussed. Theoretical results are compared to recent experimental data.

## Abstract



## NEUTRON ANGULAR DISTRIBUTION FROM HALO BREAKUP

+*Istituto Nazionale di Fisica Nucleare, Sezione di Pisa, 56100 Pisa, Italy*,  
E-mail: BONAC@MVP1.DIFI.UNIFI.IT  
†*Dipartimento di Fisica, Università di Trento, 38050 Povo, Italy and ECT\*,  
Villazzano, Trento, Italy*, E-mail: BRINK@SCIENCE.UNTN.IT

Angeila Bonacorso + and David M.Brink†

same is true for halo projectiles. In the present case  $R_s$  is the strong absorption radius with peripheral heavy-ion reactions [19,22-24]. We assume here that the strong absorption model is a well established and widely used method  $R_s$ . The strong absorption parameter greater than some strong absorption radius are those with impact parameter that the only orbits which contribute from peripheral collisions and we assume that the potential  $V_2$ . Elastic breakup arises neutron  $\Phi_2(t)$  is a continuum state in the potential  $V_2$ . The final breakup state of the is a bound state in the moving potential  $V_1$ . The final breakup state of the wave function  $\Phi_1(t)$  which can be approximated by a constant velocity path with impact parameter  $d$ .

This paper, with a light projectile and target and a high incident energy,  $s(t)$  the projectile by a moving potential  $V_1(r - s(t))$ . For the reaction studied in breakup neutron with the target is represented by a potential  $V_2(r)$  and with and the projectile core follows a classical path  $s(t)$ . The interaction of the is treated classically in Eq.(1). The target nucleus is assumed to be at rest [1,2,19-21]. The relative motion of the projectile core and the target nucleus which has been used before to discuss neutron transfer and breakup reactions [1,2,19-21].

$$A_{12} = \frac{1}{\pi} \int_{-\infty}^{\infty} dt < \Phi_2(t) | V_2(r) | \Phi_1(t) > \quad (1)$$

In the present paper the break up amplitude is calculated in time dependent perturbation theory from a formula found in a recent report [18].

More information on the present experimental and theoretical situation can be developed similar models based on the stationary scattering theory [12-17]. Serber and Glauber model [9-11] to describe the breakup. Other authors have binding of the halo nucleons. The authors of Ref. [6-8], used a version of the of other heavy-ions, but in a more extreme form because of the very weak reactions induced by a halo nucleus will have characteristics similar to those cross sections works [1-5] we have shown that the transfer to the continuum of the target, and elastic breakup. This paper is concerned with the elastic cross section is due to the sum of absorption on resonant and non-resonant states of the neutron whose single-particle  $2s_{1/2}$  wave function has a long tail. Peripheral breakup of the halo neutron in  $^{11}\text{Be}$ . This nucleus has a very loosely bound particles (cf. fragmentation reactions), 3-body physical background (transfer to the continuum reactions), halo-neutron breakup (reactions with exotic beams).

This component of the cross section can be determined experimentally from exclusive measurements of the light particle in coincidence with the ejected. Particles in which these particles are studied they have been called pre-equilibrium states in which they have corresponding to the breakup of light particles from the projectile. According to the circums- shown that a large part of the total cross section for peripheral collisions is due A number of heavy-ion reactions at intermediate and high energies have

radius for the projectile core and the target nucleus. In Ref. [22] it is given as  $R_s = r_0[(A_P - 1)^{\frac{1}{3}} + A_T^{\frac{1}{3}}]$  with  $r_0 = 1.4\text{ fm}$ .

In Eq.(1) the breakup neutron is treated quantum mechanically. Effects related to the momentum distribution of the neutron in the projectile and its final state interaction with the target are included in the wave functions  $\Phi_1$  and  $\Phi_2$ . The final state interaction of the neutron with the projectile is neglected.

There are different ways of treating the breakup wave function  $\Phi_2$  depending on the physics involved. Resonance scattering and absorption of the breakup neutron by the target has been studied by taking  $V_2$  to be an appropriate neutron-nucleus optical potential and the state  $\Phi_2$  as a neutron optical model wave function satisfying the appropriate boundary conditions [1,3,25]. When the outgoing neutron has a high energy it is often sufficient to approximate  $\Phi_2$  by a plane wave [2]. In the present paper we approximate  $\Phi_2$  by an eikonal wave function because we expect this to be a useful approach when the projectile is a halo nucleus. In fact one gets the correct free neutron scattering limit when the halo nucleus is very weakly bound. There is also a clear connection with our previous work and with simple diffraction models of breakup.

The eikonal approximation for the neutron final state wave function is [26]

$$\Phi_2^*(\mathbf{r}, \mathbf{k}_f) = e^{-i\mathbf{k}_\perp \cdot \mathbf{b}} e^{-ik_z z} e^{\frac{i}{\hbar v} \int_{+\infty}^z V_2(x, y, z') dz'} e^{\frac{i}{\hbar} \epsilon_f t} \quad (2)$$

where  $\mathbf{b}$  and  $\mathbf{k}_\perp$  are the projections of  $\mathbf{r}$  and  $\mathbf{k}_f$  on the  $xy$ -plane. The breakup amplitude can be evaluated by substituting (2) into (1) and using the bound state wave function of the neutron in the projectile transformed by a Galilean transformation for  $\Phi_1$ . The  $t$ - and  $z$ -integrals can be evaluated exactly by defining  $k_1 = -(\epsilon_i - \epsilon_f + \frac{1}{2}mv^2)/(\hbar v)$  and  $k_2 = -(\epsilon_i - \epsilon_f - \frac{1}{2}mv^2)/(\hbar v)$ , these definitions come naturally in the phases in Eq.(1) and take into account neutron recoil effects. In the final step of the calculation, which involves an integration by parts,  $k_z - k_2$  is replaced by zero. This is a good approximation for a halo nucleus because the distribution of  $k_z - k_2$  is sharply peaked around zero. The breakup amplitude is finally

$$A_{12}(\mathbf{k}_f, \mathbf{d}) = \int d\mathbf{b} e^{-i\mathbf{k}_\perp \cdot \mathbf{b}} (1 - e^{-i\chi(\mathbf{b})}) \tilde{\psi}_1(\mathbf{d} - \mathbf{b}, k_1) \quad (3)$$

where  $\mathbf{k}_\perp$  and  $k_z$  are the perpendicular and parallel directions of  $\mathbf{k}_f$  with respect to the beam direction and the Glauber phase  $\chi$  is given by  $\chi(\mathbf{b}) = \tilde{V}_2(\mathbf{b}, 0)/(v\hbar)$  where  $\tilde{V}_2(\mathbf{b}, 0)$  is the Fourier transform of the target potential in the  $z$ -direction taken at  $k_z - k_2 = 0$ .

The Glauber formula (3) includes final state interactions of the neutron with the target potential  $V_2$  in an approximate way. It is valid for high energy neutrons when the angular distribution is concentrated in the forward direction. We can understand its relation with approaches which use a plane wave final

$\rho = |(d - b)|$  and  $\eta_2 = k_z^2 - k_f^2 = k_1^2 + \eta_z^2$  where  $\eta_z = \sqrt{-2m_e/\hbar}$ . [21,27] and  $K_m$ , is a modified Bessel Function of the second kind [28]. In Eq.(5) with respect to the  $z$ -coordinate,  $C_1$  is the asymptotic normalization constant

$$\phi_{1,m_1}(r) = C_1 \eta_i^{(+)}(i\eta_r) Y_{1,m_1}(\eta_r) \quad (6)$$

where  $\phi_1$  is the Fourier transform of the asymptotic part of the initial state wave function

$$\begin{aligned} \phi_{1,m_1}(d - b, k_1) &\approx C_1 Y_{1,m_1}(k_1) e^{-\eta_r p} \left( \frac{\eta_r}{2\pi} \right)^{1/2} \\ &= 2C_1 Y_{1,m_1}(k_1) K_{m_1}(p) \end{aligned} \quad (5)$$

In the above approximation the neutron final energy dependence is contained mainly in  $\phi_1$ , which contains also the information on the momentum distribution of the neutron in the initial state. On the other hand the neutron angular distribution will be just given by the Glauuber-like amplitude which is a factor of Eq.(4), thus showing explicitly the diffractive nature of the elastic breakup. An expression similar to Eq.(4) has been recently obtained in Ref. [8], where the neutron-target rescattering was estimated by using an experimental cross section while we calculate it using an optical potential.

Eq. (3) can be simplified by using the asymptotic form for  $\phi_1$ . From the appendix to Ref. [20] we have

that the target sees the neutron bound weakly to the projectile as an incident plane wave which is scattered by the target nucleus in the usual way.

The first factor is proportional to a Glauuber amplitude for neutron elastic scat-

$$A_{12}(k_f, d) = \left[ \int dk e^{-ik_1 \cdot b} (1 - e^{-iX(b)}) \right] \phi_1(d, k_1). \quad (4)$$

There is an interesting limiting case of the amplitude and the cross-section which holds for a halo nucleus with a very weak binding. Then  $\phi(d - b, k_1)$  is a very slowly varying function of  $b$  and the integral (3) for  $A_{12}$  can be factorized

Eq.(3.1) of [2], where we studied breakup from normal nuclei). It is clear that instead of the Glauuber operator  $(1 - e^{-iX(b)})$  we get  $V_2(b, k_z - k_2)/(\nu\hbar)$  (cf. the two approaches are equivalent when  $X(b)$  is small in the region where the tail of the neutron bound state wave function extends into the region where the approximation that  $X(b)$  is small fails for an extreme halo nucleus because the expansion to first order in  $X$  and when  $k_z - k_2$  can be replaced by zero. The integral of the neutron bound state exponential in Eq.(3) can be approximated by its integrand is large so that the exponential in Eq.(3) is small in the region where the two approaches are equivalent when  $X(b)$  is clear that

state by noting that in that case the amplitude obtained is the same as (3) but

Combining Eq.(3) with Eq.(5), we get the breakup probability distribution  $d^3P(d)/dk_{\perp}dk_z = |A_{12}(k_f, d)|^2/8\pi^3$  in terms of the components of the neutron momentum and then the cross section is obtained by integration over the impact parameter  $d$  of the center of mass of the projectile relative to the target [1].

$$\frac{d^3\sigma}{dk_{\perp}dk_z} = C^2 S \int_0^{\infty} d^2 d \frac{d^3P(d)}{dk_{\perp}dk_z} P_{el}(d). \quad (7)$$

There are no interference terms from different values of  $d$  in Eq.(7) because the relative motion of the two nuclei is treated classically.  $C^2 S$  is a spectroscopic factor for the initial neutron single particle state state.  $P_{el}$  is the probability that the projectile core-target system remains in the ground state during the reaction. We suppose that the strong absorption hypothesis is a good approximation so that that  $P_{el} = 1$  for  $d > R_s$  and  $P_{el} = 0$  for  $d < R_s$ , where  $R_s$  is the strong absorption radius already discussed. One could use a smooth cut-off approximation for  $P_{el}$  as proposed in [29] but in the case of a weakly bound nucleus it gives a negligible modification to the absolute value of the cross section.

To our knowledge there have been only two attempts [7,14] to calculating the neutron angular distribution from halo breakup, which is in principle a difficult problem unless one makes several simplifying assumptions, as it is discussed in [17]. Our work can be considered as a development on these approaches [7,14] in that we use a more general form of the initial state wave function, which they both took of the Yukawa form, and an improvement on the final state wave function since ours contains final state interaction with the target via an optical potential.

Fig.(1) shows the neutron angular distribution from the reaction  ${}^9Be({}^{11}Be, {}^{10}Be){}^9Be + n$  at  $E_{inc} = 41A.MeV$  calculated with Eq.(3) averaging over the azimuthal angle  $\phi$ . The parameter values for the  $2s_1/2$  state of  ${}^{11}Be$  are  $\varepsilon_i = -0.5$  MeV,  $\gamma_i = 0.155 fm^{-1}$ ,  $C_i = 0.94 fm^{-1/2}$  and  $C^2 S = 0.77$ . Experimental points from Ref. [7] are also shown. We have used the neutron- ${}^9Be$  optical potential of [30]. In order to compare to the experimental data we have integrated the energy spectra in the range  $\varepsilon_f = 26 - 80 MeV$ . All calculations have been done at a strong absorption radius of  $R_s = 6.2 fm$ . The longdashed line is the calculation done starting from the amplitude Eq.(4) while the solid line has been obtained from the more exact form of the amplitude, Eq.(3). The results of both calculations are very similar at small  $\theta$ , where the peak in the data is due to the sum of nuclear plus Coulomb breakup [7,31]. The large angle data seem to be slightly better reproduced by the more exact calculation from Eq.(3) but due to the error bars definite conclusions cannot be drawn. The lower dotted line, dashed and upper dotted line are the neutron angular distributions  $d\sigma/\sin\theta d\theta$  for fixed values of  $\phi = 0, \pi/2$  and  $\pi$  respectively. They show that at forward angles the distribution in  $\phi$  is uniform, while there are noticeable differences for large  $\theta$ . The total elastic breakup cross section, integrated over

nucleus but goes over continuously to a breakup model which we have used function. The method is especially suited to cases where the projectile is a halo state interactions of the neutron with the target nucleus using an eliptical wave breakup from the projectile in a heavy-ion reaction. It takes into account final initial wave function of the neutron and the potential representing the target.

In this paper we have developed a diffractional model to study neutron that the source of diffraction [33] is the overlap region between the asymptotic that whole target nucleus plays the role of diffraction source while Eq.(3) shows potential of the target is spherically symmetric. In this case  $\hbar\Delta k_x \approx \hbar\Delta k_y = 177\text{MeV}/c$ . We get distributions narrower than those obtained from (3) because and out-of-plane distributions since the diffraction source represented by the wave in the incident channel and therefore gives identical forms of the in-plane amplitude Eq.(4). Eq.(4) assumes that the halo neutron behaves as a plane wave in the incident Eq.(4). By the dot line we show the  $k_x$  (or  $k_y$ ) distribution from the approximate dependence.

By the dot line we show the  $k_x$  (or  $k_y$ ) distribution from the approximation that case we get that the widths of the in-plane and out-of-plane momentum distributions can be discussed also in terms of momentum distributions. In that case values agree with those estimated in [32]. The in-plane momentum distributions  $k_x$  are not symmetrical around  $k_x = 0$  because of a slight non-uniform dashed line respectively) are very close to each other. They were obtained from Eq.(7) after integration over  $k_z$ . We get in fact  $\hbar\Delta k_x \approx \hbar\Delta k_y = 187\text{MeV}/c$ .

Distribution,  $dr/dk_x$ ,  $dr/dk_y$  for the same reaction, shown in Fig.(3) (solid and that case we get that the widths of the in-plane and out-of-plane momentum distributions car be discussed also in terms of momentum distributions. In that case we get that the widths of the in-plane and out-of-plane momentum distributions are not symmetrical around  $k_x = 0$  because of a slight non-uniform to the beam pointing away from the target.

Our results can be discussed by it having the final momentum component perpendicular forward angles. The slow neutrons interact instead with the target potential do not suffer much interaction with the target potential and fly away at very physical interpretation of these results is that the neutrons with high final energy the neutron final energy to values larger than the beam energy per nucleon. The line), from Eq.(3), and they disappear progressively increasing  $\phi$  and increasing line, from Eq.(3), and they disappear also in the calculation for fixed  $\phi = 0$  (bottom smooth.

Diffraction oscillations appear also in the calculation for fixed  $\phi = 0$  (bottom calculation the surface of the target nucleus which is diffractioning the neutrons is imum is very small and cannot be noticed in the figure. This is because in our  $(J_1(k_1 R_3)/k_1 R_3)^2$ . The difference between the minimum and secondary maximum at  $\theta \approx 64^\circ$  and  $\theta \approx 86.5^\circ$  in accord with a cross section proportional to calculation from Eq.(4) has a first minimum and a secondary diffractional maximum at  $\theta \approx 64^\circ$ , and  $\theta \approx 86.5^\circ$  in result of the calculation from Eq.(4). The over  $\phi$  while the dashed line is the result of the calculation averaged over  $\phi$  to  $\phi = \pi$ , and 0 respectively. The dotted line is the calculation solid lines correspond to  $\phi = \pi$ , and 0 respectively. The top and bottom solid lines correspond to the incident beam energy per nucleon. The top and bottom solid lines correspond to the incident beam energy per nucleon for a fixed neutron final energy equal to [7] where it was found  $a_{10Be + n} = 0.24 \pm 0.056$ .

energies and angles, is  $\phi_c = 0.236$ , in good agreement with the results of Ref.

before for normal heavy ions where the neutron binding energy is several MeV. It can be used to calculate angular distributions of the breakup neutron as well as the distributions of longitudinal and transverse momenta. Furthermore the method allows for the description of the scattering out of the reaction plane, which is not uniform. A simple limiting case of our transition amplitude valid in the case of very weak binding and almost constant tail of the halo wave function has been discussed in connection to the application of the model to the breakup of  $^{11}Be$  on a light  $^9Be$  target. It consists in considering the neutron re-scattering on the target as that of an initial plane-wave. The two formulas describe equally well the small angle scattering but they give slightly different results at large angles. As a consequence the transverse momentum distributions of the halo neutrons from Eq.(1) are similar to, but somewhat broader than the corresponding transverse momentum distributions for neutron free scattering by the target nucleus (cf. [34]). The method presented in this paper can be used also to calculate the neutron energy spectra and related parallel momentum distribution [5].

One of us (A.B.) is very grateful to G.Hansen for several discussions and comments during the preparation of this work. She wishes also to thank E. Piasecki for a critical reading of the manuscript.

- [1] A.Bonacorso and D.M.Brink, Phys. Rev. C38, 1776 (1988).
- [2] A.Bonacorso and D.M.Brink, Phys. Rev. C43, 299 (1991).
- [3] A.Bonacorso and D.M.Brink, Phys. Rev. C44, 1559 (1991).
- [4] A.Bonacorso and D.M.Brink, Phys. Rev. C46, 700 (1992).
- [5] A.Bonacorso and D.M.Brink, Preprint IFUP-TH 3A/97.
- [6] A.Amne et al., Phys.Lett. B250, 19 (1990).
- [7] R.Amne et al., Nucl.Phys. A575, 125 (1994).
- [8] P.G.Hansen , Phys.Rev.Lett. 77, 1016 (1996).
- [9] R.Serber, Phys.Rev. T2, 1008 (1947).
- [10] R.J.Glauber, Phys.Rev. 99, 1515 (1955).
- [11] R.J.Glauber, *High-Energy Collision Theory, Lectures in Theoretical Physics*, Interscience, New York, 1959) page 315.
- [12] C.A.Bertulani and K.W.Mc Voy, Phys. Rev. C46, 2638 (1992).
- [13] Y.Ogawa,K.Yabana, and Y.Suzuki, Nucl. Phys. A543 (1992) 722.
- [14] F.Barranco, E.Vigezzi and R.A.Brogilla, Phys.Lett. B319, 387 (1993).
- [15] H.Sagawa and N.Takiyawa, Phys. Rev. C50, 985 (1994).
- [16] A.A.Korschennikov and T.Kobayashi , Nucl.Phys. A 576, (1994) 97.
- [17] K.Hencken, G.Bertsch and H.Esbensen, Phys.Rev. C54, 3043, (1996).
- [18] P.G.Hansen, A.S.Jensen and B.Johnson, Ann.Rev. Nucl. Part. Sci. 45, 591 (1995).
- [19] R.A.Brogilla and A.Wimther, "Heavy Ion Reactions: Lectures Notes", 2nd Edition, Addison-Wesley, 1991, Redwood City, Calif.
- [20] L.Lo Monaco and D.M.Brink, J.Phys.G 11, 935 (1985).
- [21] A.Bonacorso, G.Piccolo and D.M.Brink, Nucl.Phys. A441, 555 (1985).

## References

- [22] D.M.Brink, *Semiclassical Methods in Nucleus-Nucleus Scattering*, Cambridge University Press, Cambridge, 1985. Pag.19.
- [23] G.R.Satchler, *Direct Nuclear Reactions*, Clarendon Press, Oxford 1983.
- [24] R.Bass, *Nuclear Reactions with Heavy-Ions*, Springer Verlag, Berlin 1980.
- [25] A.Bonaccorso, I.Lhenry and T. Süomijarvi, Phys.Rev. C49 , 329 (1994).
- [26] A.Bonaccorso, Phys.Rev. C53, 849 (1996).
- [27] Fl.Stancu and D.M.Brink, Phys.Rev. C32, 1937 (1985).
- [28] I.S. Gradshteyn and I.M.Ryzhik, *Table of Integrals, Series and Products*, Academic Press, New York, 1980. Pag.952.
- [29] A.Bonaccorso,D.M.Brink and L.Lo Monaco, J.Phys.G13,1407 (1987) .
- [30] J.H.Dave and C.R.Gould, Phys. Rev. C28,2212 (1983).
- [31] J.Margueron, A.Bonaccorso and D.M.Brink, in preparation.
- [32] P.G.Hansen, Nucl.Phys. A588, 1c (1995).
- [33] J M.Cowley, *Diffraction Physics*, North-Holland Publishing Company, Amsterdam,Oxford, 1985.
- [34] P.G.Hansen, Proceedings of the International Conference on Exotic Nuclei and Atomic Masses, Arles, France, June 1995.

**Fig.1.** Angular distribution of the one-neutron breakup in the reactions  ${}^9Be({}^{11}Be, {}^{10}Be){}^9Be + n$  at  $E_{in} = 41A. MeV$ . The solid and longdashed lines are calculations using Eqs.(3) and (4) respectively, averaged over the azimuthal angle  $\phi$ . The bottom dot line, short dashed and upper dot lines are the neutron angular distribution for fixed values of  $\phi$ ,  $\phi = 0, \pi/2$  and  $\pi$  respectively.

**Fig.2.** Calculations of the neutron angular distribution for a fixed neutron final energy equal to the incident beam energy per nucleon for the same reaction as Fig.(1). The top and bottom solid lines correspond to  $\phi = \pi$ , and 0 respectively. The dot line is the calculation averaged over  $\phi$  while and 0 respectively. The dot line is the calculation averaged over  $\phi$  while from Eq.(3), for the same reaction as Fig.(1), after integration over the two other directions. Shortdashed line is calculated from Eq. (4).

**Figure captions**

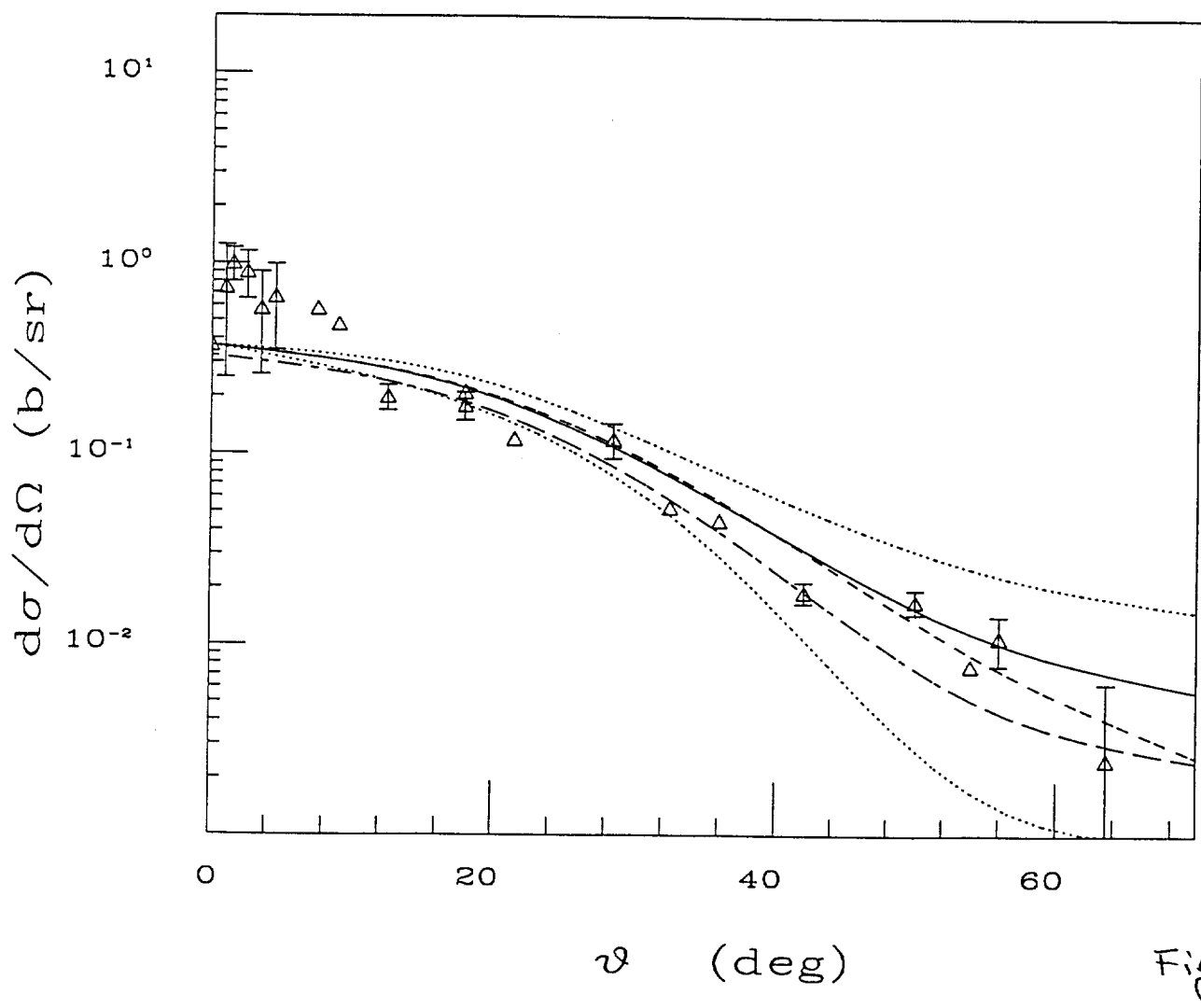
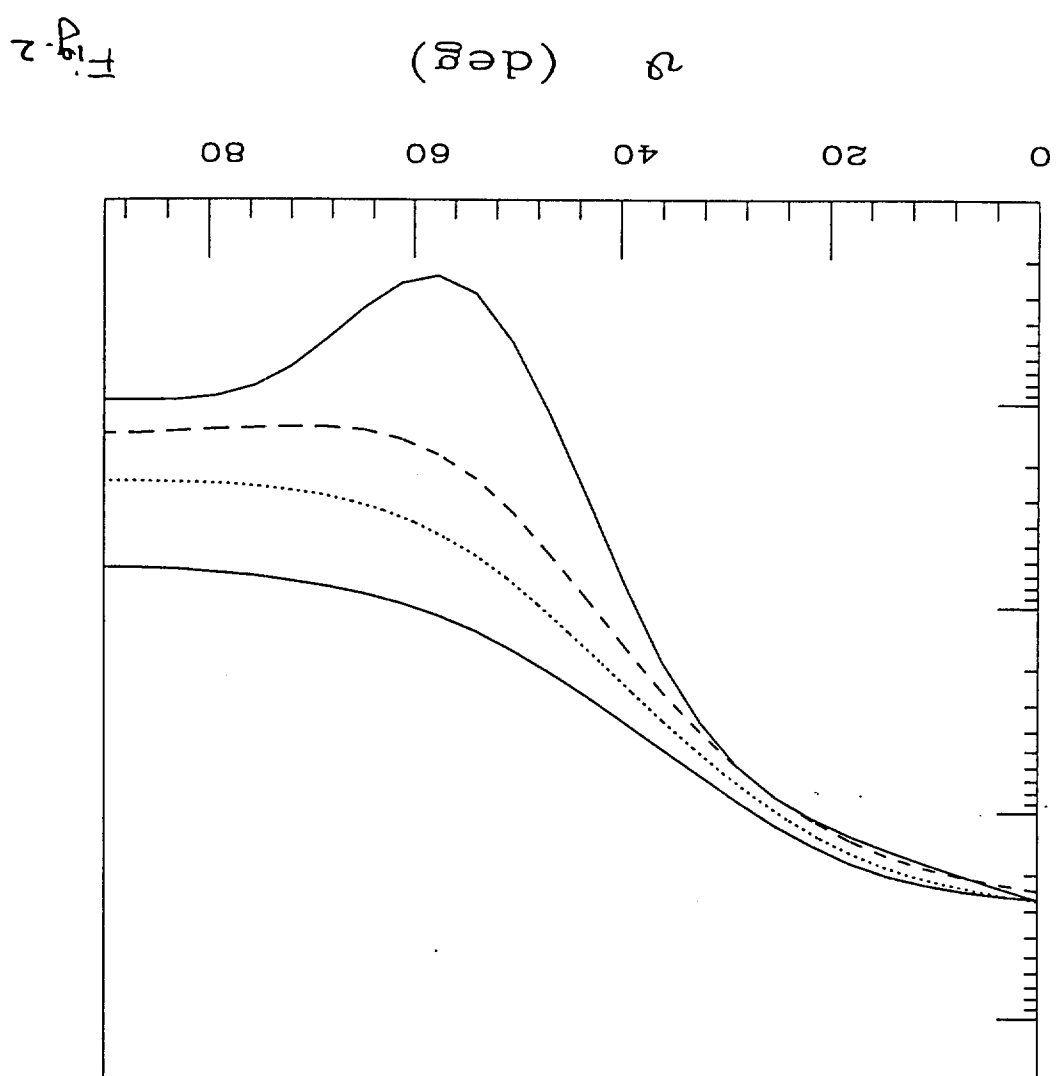


Fig. 1

$d\sigma/d\Omega$  (arb. units)

$10^{-3}$   
 $10^{-2}$   
 $10^{-1}$   
 $10^0$



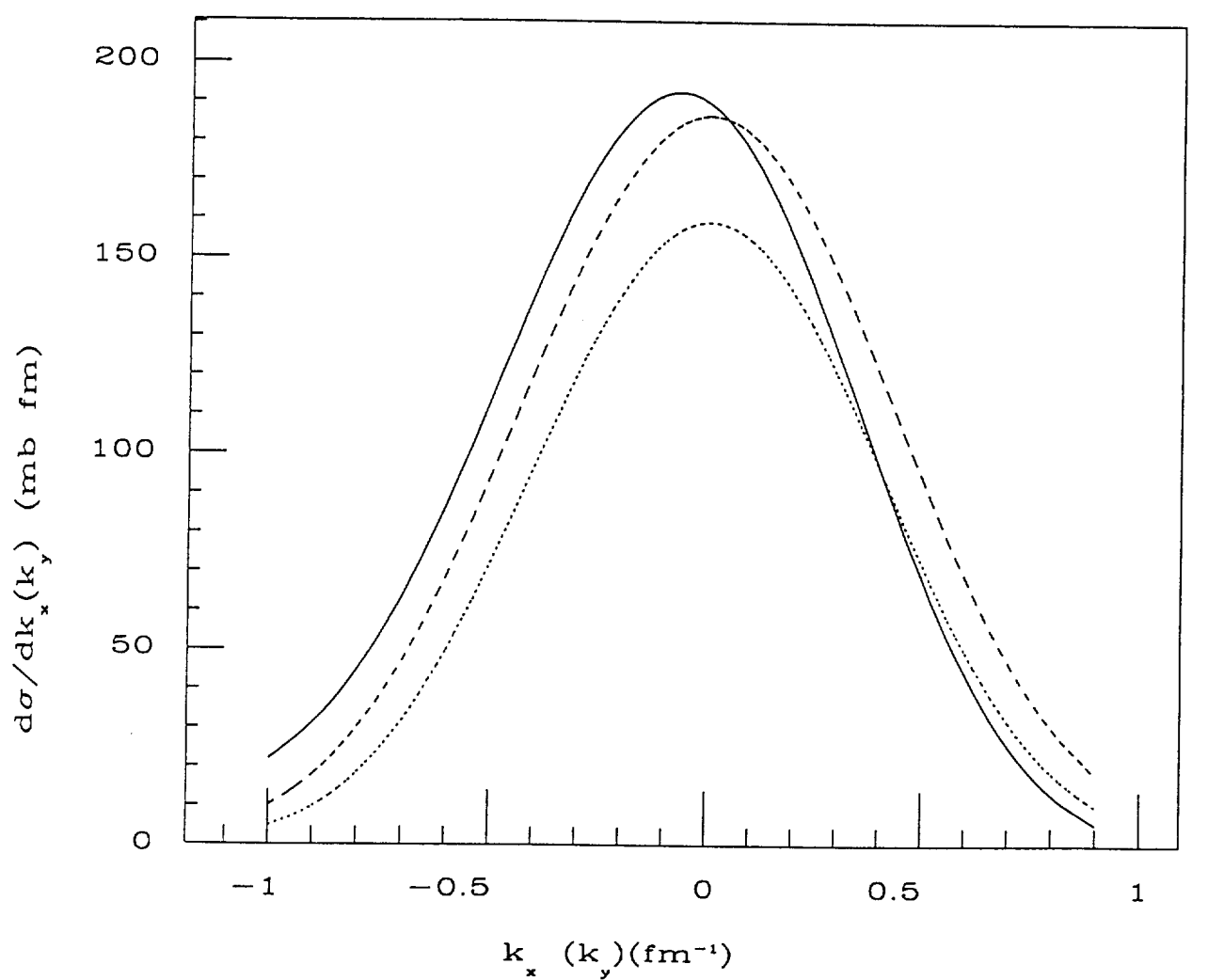


Fig. 3